

Mutational Analysis of *Citrus viroid III* Symptom Expression

R. A. Owens¹, S. M. Thompson¹, P. J. Sieburth², and M. E. Hilf³

¹Molecular Plant Pathology Laboratory, USDA/ARS, Beltsville, MD 20705, USA;

²Bureau of Citrus Budwood Registration, Winter Haven, FL 33881, USA;

³USDA, ARS, Horticultural Research Laboratory, Fort Pierce, FL 34945, USA

ABSTRACT. Close planting of viroid-infected citrus growing on trifoliate orange or trifoliate hybrid rootstocks has been shown to increase fruit yield and lower production costs. We would like to adapt *Citrus viroid III* (CVD-III) for use with other rootstocks and, toward that end, have examined the effect of introducing sequence changes in the lower portion of its central conserved region on replication and symptom expression in Etrog citron. Mutations at positions 173-174 and 179-181 appeared to be essentially neutral, having little or no effect on foliar symptoms. The effects of deletions affecting positions 53-54 in the pathogenicity domain were more complex. Like the corresponding portion of *Potato spindle tuber viroid* (PSTVd), the central conserved region of CVD-III contains a putative loop E motif. Unlike PSTVd, however, mutagenesis of CVD-III positions 189-191 failed to yield any stable sequence variants. Results from UV cross-linking experiments indicate that there are significant differences between the three-dimensional structures of the loop E motif in these two viroids. Understanding the effects of these structural differences on viroid replication may allow us to generate CVD-III variants having altered host range and dwarfing properties.

More than 30 yr of field studies carried out in Australia (reviewed in 9), California (18-20), Europe (22), and Israel (1) have shown that graft-transmissible viroid dwarfing can be used to control tree size in intensive citrus plantings. After a lag period of 3-5 yr, trees growing on trifoliate orange or citrange rootstocks and inoculated with viroid(s) during their first year in the field exhibited greatly reduced vegetative growth during the summer and autumn with no effect on spring flush growth and fruit set. Advantages of high density citrus planting include improved early return on investment, more efficient use of resource inputs, and lower harvesting costs (9).

Citrus producers in Florida are facing increasing economic pressures, and viroid-induced dwarfing offers one possible strategy to reduce labor costs. We have recently initiated a field study to determine the feasibility of using naturally occurring strains of *Citrus viroid III* (CVD-III) to dwarf Valencia sweet orange and grapefruit scions grow-

ing under subtropical conditions. While awaiting results from this field study, we have begun to systematically screen mutagenized populations of CVD-IIIa and CVD-IIIb for novel variants that will be more effective dwarfing agents for newer rootstocks now coming into use in Florida (13). For such a strategy to be successful, mutagenesis targets should include those portions of the viroid that modulate replication and viroid-host interaction.

One method to identify promising targets for mutagenesis takes advantage of the pattern of natural sequence variation. To date, more than 50 different sequence variants of CVD-III have been described, and two variants, CVD-IIIa (16) and CVD-IIIb (21) dominate the quasispecies. The three-dimensional structure of viroids and other RNA molecules is also shaped by the presence of various sequence motifs, specific tertiary interactions that involve ordered arrays of non Watson-Crick base pairs (10). One such motif is the UV-sensitive "loop E motif" first found in *Escherichia coli*

5S rRNA. This motif is now known to be widely distributed among both prokaryotic and eukaryotic RNAs, including PSTVd (2) and several other subviral RNAs (10), and sequence changes in the loop E motif of PSTVd lead to dramatic alterations in both host range (24) and symptom expression (15).

This report describes results from four independent screens of CVd-III mutant libraries. Two screens were focused on a putative loop E motif located in the central conserved region of CVd-IIIb; the remaining screens explored the effects of sequence changes in the adjoining portions of the molecule. Several novel variants were recovered, but none induced foliar symptoms that were more severe than those of wild-type CVd-IIIa or CVd-IIIb.

MATERIALS AND METHODS

Mutagenesis of infectious CVd-III RNA transcripts. We have previously described the construction of an expression cassette that allows the *in vitro* synthesis of infectious, precisely-full-length CVd-III RNA transcript by ribozyme cleavage (11). Mutations were introduced into the lower portion of the CVd-IIIa and -IIIb central conserved region using an overlap extension strategy (6) and four pairs of degenerate oligonucleotide primers: 5'-ATCCTCCGGCWKACCKYYWTCA GCWCGCCGCTAGTCG-3' (CVd-IIIa positions 163-200) and 5'-CGACTA-GCGGCGWGCTGAWRRMGGGTM WGCCGGAGGAT-3' (complementary to CVd-IIIa positions 200-163); 5'-ATCCTCCGGCWKACCKYYWAGCWCC-GCTAGTCG-3' (CVd-IIIb positions 163-197) and 5'-CGACTA-GCGGCGWGCTWRRMGGGTMWGC CGGAGGAT-3' (complementary to CVd-IIIb positions 197-163); 5'-CCTTCTAGCTCCNNNTAGTCGAG CGGA-3' (CVd-IIIb positions 177-203) and 5'-TCCGCTCGACTANNNGGAGCTAGAAGG-3' (complementary to CVd-IIIb positions 203-177);

and 5'-CCTTCTAGCTCCNNNTAGTCGAGCGGA-3' (CVd-IIIb positions 177-203) and 5'-TCCGCTCGACTA-ANNNGGAGCTAGAAGG-3' (complementary to CVd-IIIb positions 203-177). Mixed bases are indicated by the following codes: N = A+C+G+T; K = T+G; M = A+C; R = A+G; W = A+T; and Y = C+T. Mutagenesis efficiency was monitored by automated sequence analysis of the reassembled CVd-IIIa or CVd-IIIb cDNAs prior to transcription.

Characterization of CVd-III sequence variants. Bioassays of mutagenized CVd-III RNA transcripts were carried out as previously described (13). Mixtures containing 16-128 different sequence variants (number of variants determined by the degeneracy of the primers used for mutagenesis) were slash inoculated into groups of 20-25 rooted Etrog citron cuttings (clone RMA 861-S1) at concentrations sufficient to infect approximately 90% of the plants. Inoculum concentrations ranged between 8-64 ng ribozyme-cleaved CVd-III RNA/ μ l (depending again on the number of sequence variants in the mixture).

Approximately 3 weeks post-inoculation (pi), the plants were cut back and allowed to grow out for 4-8 mo before initial symptom assessment. Four aspects of symptom expression were assessed using a numerical rating system. Three aspects, vein splitting, veinal necrosis, and petiole necrosis, were scored as either present (1) or absent (0). Leaf epinasty was scored as severe (3), moderate (2), mild (1), or absent (0). The plants were then cut back a second time and allowed to re-grow for an additional 4 mo before symptoms were reassessed. CVd-III progeny present at the time of the first symptom assessment were characterized by RT-PCR and automated sequence analysis of the resulting uncloned viroid cDNAs using primers C2' (5'-ACTTCCGTCTTTACTCCAC-3', complementary to CVd-

IIIb positions 138-119) and H2' (5'-CTCCGCTAGTCGGAAAGACT-3', CVd-IIIb positions 139-158).

Effect of CVd-III infection on root development. To evaluate the possible inhibitory effects of CVd-III infection on root development, groups of 6-7 approximately 1-yr-old Carrizo citrange and Rangpur lime seedlings growing in 1-gallon (approx. 3.8 liter) pots containing a 2:1 (v/v) mixture of MetroMix 510 and perlite were graft-inoculated with bark tissues harvested from Etrog citron infected with either CVd-IIIa or CVd-IIIb (2 buds/plant). The grafts were unwrapped approximately 4 weeks post inoculation, and the plants were transferred to 1.5-gallon pots and maintained under the high light-warm temperature conditions favoring viroid replication. Plants were irrigated with a water-soluble fertilizer (Peters Excel 21-5-20-W.R. Grace, Fogelsville, PA) solution supplemented with Sprint 330 (Becker Underwood, Ames, IA) and CuSO₄ (Sigma-Aldrich) applied with a proportioner at a rate of 100 ppm N, 6 ppm Fe, 2 ppm Cu, and were then periodically cut back to encourage symptom development. Effects of viroid infection on shoot and root development were evaluated approximately 21 mo pi.

UV cross-linking and TGGE analysis. As described above, overlap extension mutagenesis was used to introduce a series of sequence changes into the loop E motif of a PSTVd "mini-RNA" (17). The net effect of these changes was to convert this portion of the molecule into a structure virtually identical to the loop E motif of CVd-IIIb. Polyacrylamide gel-purified mini-RNAs were slowly renatured under high ionic strength conditions (i.e., 4 M urea, 400 mM NaCl) to favor Loop E formation, and small aliquots (5 µl) were placed on a piece of Parafilm floating on an ice-water bath and irradiated with short wave length UV light for 2-5 min in a Stratagene Model 1800 Stratalinker. Following

UV irradiation, three volumes of loading dye (9 M urea, 0.2× TBE buffer containing bromphenol blue and xylene cyanole FF) were added and the extent of UV cross-linking assessed by electrophoresis in 7.5% polyacrylamide gels (39:1, acrylamide:bis-acrylamide, w/w) containing 1× TBE buffer and 8 M urea, and run at 55°C. Temperature gradient gel electrophoresis of non-crosslinked miniRNAs was carried out in 7.5% polyacrylamide gels (29:1, acrylamide:bis-acrylamide, w/w) containing 0.2× TBE buffer, 5 mM NaCl (8).

Nucleotide sequence analysis. Sequences of previously described CVd-III variants were retrieved from the Subviral RNA Database (<http://subviral.med.utoronto.ca/cgi-bin/home.cgi/oldURL=1>). Multiple sequence alignments were generated with the Clustal V program implemented through the Megalign function of the Lasergene software package (Version 4.0—DNASTAR). Minor adjustments were manually introduced into the final alignment to maximize sequence homology and duplicate sequences were discarded, resulting in a collection of 47 non-redundant CVd-III sequences (June, 2003). Structural calculations were performed with *mfold* Version 3.1 as implemented on the *mfold* server [25; <http://www.bioinfo.rpi.edu/applications/mfold/old/rna/>].

RESULTS

As shown in Fig. 1, CVd-IIIa (297 nt; GenBank Accession S76452) and CVd-IIIb (294 nt; GenBank Accession S75465) differ at a total of 13 positions; with 10 substitutions and three insertions. Figure 2A shows the distribution of sequence changes between the 47 different CVd-III variants with respect to the central conserved region of CVd-IIIb. The relative positions of the two sets of changes introduced into the lower portion of the CVd-IIIb central con-

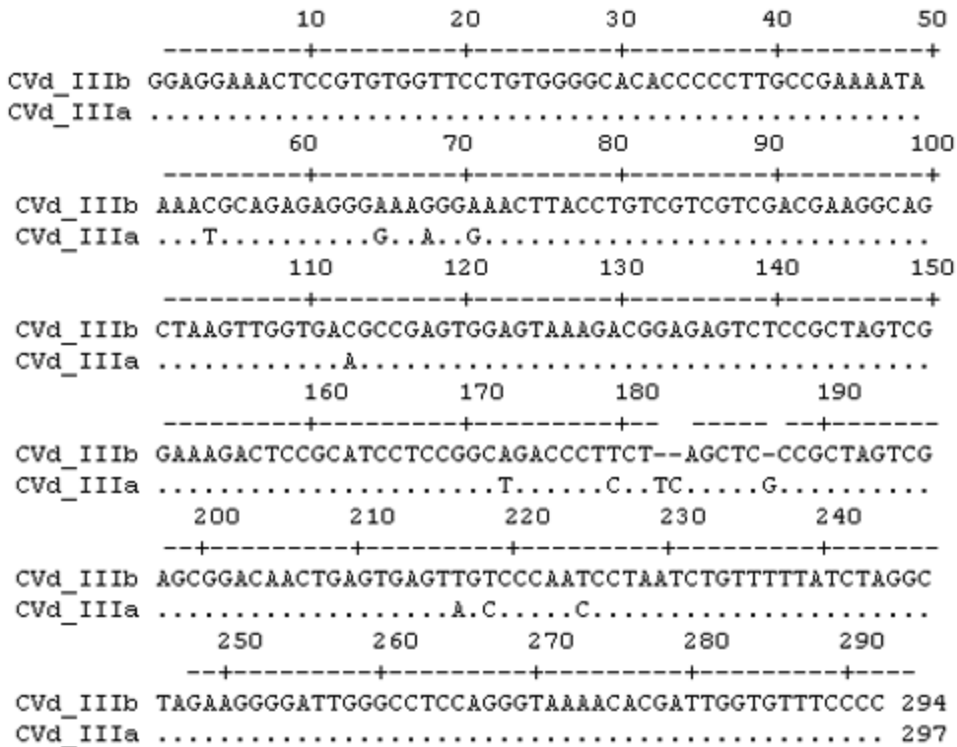


Fig. 1. Nucleotide sequences of CVd-IIIa (297 nt) and CVd-IIIb (294 nt). Locations of the 10 substitutions and three insertions (positions 182a, 182b, and 187a) that distinguish these two variants are shown.

served region and the putative loop E motif are shown in Fig. 2B. Figure 2C compares the structure of the loop E motifs of PSTVd and CVd-III in greater detail, with special emphasis on the relative positions of non Watson-Crick base pairs. Although similar in overall sequence, note that the putative CVd-III loop E motif contains a very different array of potential non Watson-Crick base pairs. Locations of a C/U substitution that allows PSTVd to replicate freely in tobacco (24) and a nearby U/A substitution that is responsible for a “flat top” phenotype in Rutgers tomato (15) are marked.

Effects of mutations in the lower portion of the CVd-III central conserved region. Our attempts to improve the dwarfing properties of CVd-III employed two complementary mutagenesis strategies. In experiments 1 and 2, we

examined the effect of partially randomizing positions flanking the putative loop E motif of CVd-IIIa and CVd-IIIb. To lessen the chance that wild-type viroid would overgrow viable variants, a pair of attenuating mutations (11, 13) was introduced at positions 44 and 54. Experiments 3 and 4 examined the effect of mutagenizing the loop E motif itself. In experiment 3, CVd-IIIb positions 189-191 were randomized after introducing attenuating mutations at positions 44 and 54. In experiment 4, the C residue at position 191 was changed to a U and only positions 189 and 190 were randomized.

Characterization of the progeny from individual infected plants revealed the presence of several novel sequence variants, and the results from all four bioassays are summarized in Table 1. For each experiment, the sequence changes

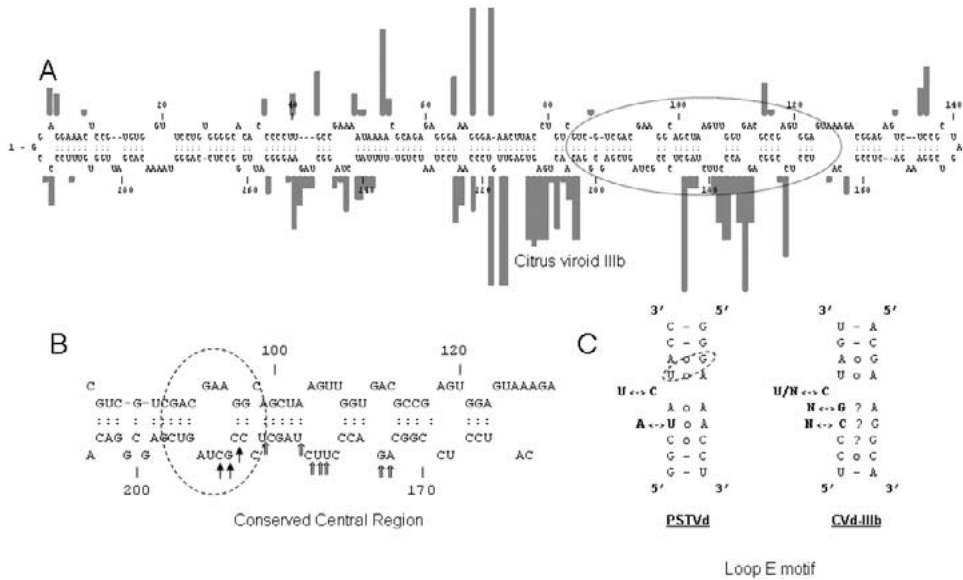


Fig. 2. Mutagenesis of the CVd-III central conserved region. (A) Unbranched, near-lowest free energy structure of CVd-IIIb showing the variability observed among 47 infectious sequence variants. Bar heights indicate the relative amount of variation at individual nucleotide positions. (B) Enlarged view of the central conserved region and flanking sequences showing the relative positions of a putative loop E motif (dashed circle). \uparrow , sequence variation between CVd-IIIb and CVd-IIIa; \uparrow , sequence changes introduced site-directed mutagenesis. (C) Comparison of the loop E motifs of PSTVd (left) and CVd-IIIb (right). Positions of established (open circles) and potential (question marks) non-Watson-Crick base pairs as well as the UV-induced cross-link in PSTVd (dashed circle) are shown.

detected in the progeny are boxed. The sequence above each box is the sequence of the respective inoculum. The sequence of CVd-IIIb is provided as a reference (Fig. 1).

Identification of CVd-III variants. In experiment 1, all 25 plants inoculated with a mixture of attenuated CVd-IIIb variants became infected. Only a small minority (3 of 25 plants) contained progeny with mutations in the lower central conserved region, however. A similar pattern was observed in experiment 2 where the inoculum contained a comparable mixture of 128 attenuated CVd-IIIb variants. Why so few of the plants inoculated in this experiment became infected is unclear, but the progeny contained only mutations derived from the attenuating changes at positions 44 and 54.

Mutagenesis of the putative loop E motif in CVd-IIIb failed to yield

any sequence changes affecting positions 189-191. In experiment 3, progeny resulting from the randomization of all three positions included two variants containing spontaneous changes related to the attenuating mutation at position 54. Comparable results were also obtained in experiment 4 where a C/U substitution was introduced at position 189 before positions 190 and 191 were randomized. Note, however, that one or more infected plants in experiments 3 and 4 were found to contain CVd-IIIa. CVd-IIIa differs from CVd-IIIb at a total of 13 positions, only one of which (position 54) was targeted by our mutagenesis strategy.

Effect of sequence changes on CVd-III foliar symptoms. As described in Materials and Methods, the foliage of infected plants was examined for any increase in symptom severity that might signal the

TABLE 1
SEQUENCE VARIANTS RECOVERED AFTER CVd-III MUTAGENESIS

Progeny	Mutants	IIIb	IIIa	Targeted positions ^a																	Spontaneous changes
				44	54 ^a	173 ^a	174	179	180 ^b	181	182	186	189	190	191						
				G	C/U	A/U	G	U	U/C	C	U	U	C	G	C						
<i>Experiment 1</i> [25 plants—CVd-IIIa]																					
	8	0	1	A	U	W	Y	K	Y	Y	W	W									
	7			A																	
	1			A													-A53				
<i>Experiment 2</i> [25 plants—CVd-IIIb]																					
	25	0	0	A	U	W	K	K	Y	Y	W	W									
	13			A																	
	1			A													-A53				
	9			A																	
	1			A													-A53				
	1			A																	
<i>Experiment 3</i> [25 plants—CVd-IIIb]																					
	22	2	1	A	U								N	N	N						
	18			A																	
	3			A													-A53				
	1			A													-A53, -A54				
<i>Experiment 4</i> [20 plants—CVd-IIIb]																					
	0	16	4										N	N	N						

Data are expressed as no. infected plants containing individual sequence variants. The number of plants inoculated in each experiment is shown in brackets. Mixed bases in the inocula are indicated by the following codes: N = A+C+G+T; K = T+G; M = A+G; W = A+T; and Y = C+T.

^aThe sequence of CVd-IIIb is provided as reference (see Fig. 1). At positions where the sequences of CVd-IIIa and IIIb differ, the nucleotide present in CVd-IIIb is shown first.

presence of variant(s) with improved dwarfing properties. A number of plants initially appeared to be severely stunted (see Fig. 3), but these differences did not persist after cutback and re-growth. Also, sequence analysis of uncloned RT-PCR products failed to reveal any correlation between stunting and nucleotide sequence of the progeny (results not shown). A more thorough, numerical evaluation of other symptoms of CVd-III infection did, however, reveal certain differences between the symptoms of wild-type CVd-III infection and those induced by certain variants. The data from this analysis are summarized in Table 2.

Each infected Etrog plant was evaluated for four different aspects of CVd-III symptom expression; vein



Fig. 3. Foliar symptoms of CVd-III infection in Etrog citron. Photograph was taken approximately 5 mo after slash inoculation and 4 mo after initial cutback. Healthy, uninoculated control; IIIa and IIIb, plants containing wild-type CVd-IIIa or CVd-IIIb, respectively; G44A + C54U, two plants that contain a CVd-IIIb variant with attenuating mutations at positions 44 and 54. Note that the marked stunting of the leftmost plant in this pair was not accompanied by a comparable increase in leaf epinasty.

splitting, veinal necrosis, petiole necrosis, and leaf epinasty. The degree of leaf epinasty represents as much as 50% of the resulting total score, but most of the values reported in Table 2 are averages derived from two or more plants. Several conclusions can be drawn about the effect of specific sequence changes. First, variants containing substitutions at positions 44 and 54 induced symptoms that were considerably milder than those produced by wild-type CVd-IIIa or CVd-IIIb. This decrease was due mostly to a marked reduction in leaf epinasty. Second, additional changes at positions 173 and 180-182 was not able to overcome the attenuating effects of mutations at positions 44 and 54. Third, deletion of an A residue at position 53 intensified symptom expression with variants of both CVd-IIIa and -IIIb. And finally, deletion of the neighboring cytosine residue at position 54 appeared to have just the opposite effect.

Effect of CVd-III infection on root development. Because field studies had shown both Carrizo citrange and Rangpur lime rootstocks to be susceptible to viroid dwarfing (9), we decided to examine the response of young Carrizo and Rangpur seedlings growing in the greenhouse to CVd-III infection. Twenty one months after graft inoculation with either CVd-IIIa or CVd-IIIb, no symptoms of viroid infection were visible in the above-ground portions of the inoculated plants. This lack of symptom expression was not due to the absence of viroid, because RT-PCR analysis revealed all grafted plants to be infected (results not shown). Visual comparisons of healthy and viroid-infected root systems suggested, however, that CVd-III infection may inhibit root development.

To examine this effect in greater detail, we compared the mean root dry weights for each treatment. CVd-III infection appeared to be associated with a small (12-17%) decrease in root dry weight, but the

TABLE 2
EFFECT OF CVD-III SEQUENCE CHANGES ON SYMPTOM EXPRESSION IN ETROG CITRON

Progeny sequence	# trees	Symptom severity ^a				Total
		Vein splitting	Veinal necrosis	Petiole necrosis	Epinasty	
CVD-IIIb						
Wild-type	15	1	1	1	2.87	5.87
Revertants ^b	18	1	1	1	2	5.00
44 ^c 54	31	0.94	0.29	0.93	0.32	2.48
44 54 173	9	0.77	0.33	1	0.22	2.32
44 -53 54 173	1	1	0	1	1	3.00
44 -53	2	1	0.50	1	1	3.50
44 -53 (partial)	2	1	0	0.50	1	2.50
44 -53 -54	1	1	0	1	0	2.00
44 54 173	1	0	0	1	1	2.00
180 181 182						
CVD-IIIa						
Revertants ^b	6	1	1	1	2.17	5.17
44	6	0.50	0.66	0.83	0.66	2.65
44 (50%)	1	0	1	1	1	3.00
44 -53	1	1	1	1	1	4.00

^aSymptom expression was assessed numerically as described in Materials and Methods. Values shown are averages.

^bPlants were inoculated with a mixture of sequence variants but the progeny contained only wild-type CVD-III.

^cPositions of sequence change(s) in individual variants derived from either CVD-IIIa or CVD-IIIb are listed. -, nucleotide deleted in progeny.

small sample size (≤ 7 plants/treatment) and larger-than-expected variability within treatments prevented any firm conclusions.

Susceptibility of the CVD-III loop E motif to UV crosslinking.

As shown in Fig. 2C, the loop E motifs of PSTVd and CVD-III contain different arrays of potential non Watson-Crick base pairs below the bulged C residue shown on the left side of each structure. Particularly noteworthy are i) the substitution of a GoA pair for the AoA pair immediately below the bulged C residue and ii) the possible presence of two Watson-Crick C-G base pairs just below the GoA pair. To determine the possible effects of these changes on the overall conformation of loop E, we compared the ability of UV irradiation to cross-link PSTVd and CVD-III mini-RNAs.

Following slow renaturation in a high ionic strength buffer that

favors loop E formation, the two mini-RNAs were irradiated with short wave length UV light and analyzed by PAGE under denaturing conditions. As shown, the loop E motif of CVD-III (Fig. 4A) was highly resistant to UV cross-linking (Fig. 4B). Cross-linked RNAs formed by UV irradiation of mini-PSTVd have a lariat conformation and migrate more slowly than the corresponding linear RNAs (compare lanes 2-4). Comparison of lanes 6-7 with lane 5 showed that replacing the non Watson-Crick GoA pair immediately below the bulged C at position 191 in CVD-III with an AoA pair results in a definite (albeit modest) increase in UV susceptibility.

DISCUSSION

Efforts to increase citrus production/profitability through the use of viroid-induced dwarfing have been

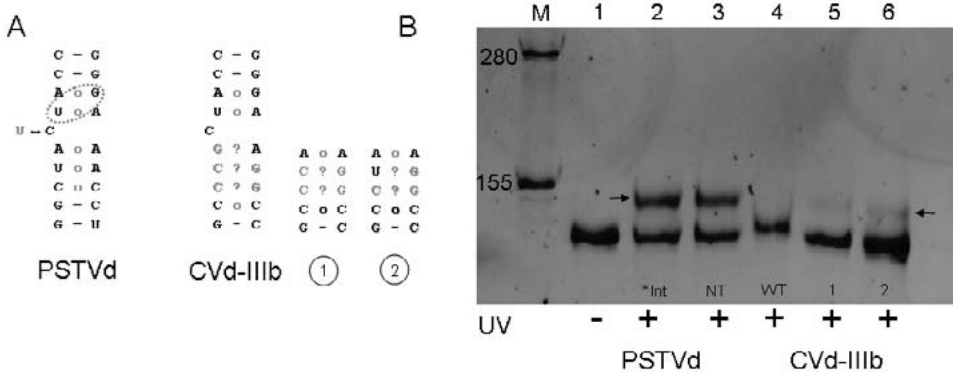


Fig. 4. UV-induced crosslinking of the PSTVd and CVd-IIIb miniRNAs. (A) Comparison of the loop E motifs of PSTVd (left) and CVd-IIIb (right). Positions of known (open circles) and potential (question marks) non-Watson-Crick base pairs as well as the UV-induced cross-link in PSTVd (dashed circle) are shown. (B) Denaturing PAGE analysis of cross-linked PSTVd and CVd-IIIb miniRNAs. Lane M, linear RNA markers (Invitrogen); lanes 1-2, mini PSTVd-Int; lane 3, mini PSTVd-NT where the bulged C has been replaced by U residue; lane 4, mini CVd-IIIb; lane 5, mini CVd-IIIb containing a GoA → AoA double mutation immediately below the bulged C residue; and lane 6, mini CVd-IIIb containing an additional C → U substitution at position 189. Samples marked with a “+” were irradiated with short wave length UV light for 5 min.

hampered by the lack of a suitable screening assay to rapidly assess the dwarfing potential of specific viroid/rootstock combinations. Field trials take several years for initial evaluation, and opportunities to monitor the physiological changes associated with viroid infection are limited (9). The CVd-III mutant screens described above were carried out by monitoring the foliage of Etrog citron indicator plants for visible changes in symptom expression over a 9-12 mo period.

Mutagenesis of the lower central conserved region of CVd-III yielded several novel variants, but in no case were foliar symptoms more severe than those induced by the wild-type viroids. As previously reported (11), the presence of a G/A substitution at position 44 resulted in a marked attenuation of symptom expression, but the effects of changes at positions 53 and/or 54 were more variable. The size and nucleotide composition of a small potential bulge loop involving position 54 appears to have a major effect on symptom expression in the foliage. In contrast, changes affect-

ing positions 173 and 180-182 appeared to be essentially neutral.

As shown in Figs. 2C and 4A, the putative loop E motifs of CVd-III and PSTVd contain quite different arrays of potential non Watson-Crick base pairs. Particularly noteworthy are i) the substitution of a GoA pair for the AoA pair immediately below the bulged C residue and ii) the possible presence of two Watson-Crick C-G pairs just below this GoA pair in CVd-III. Results from our UV cross-linking experiments indicate that the tertiary structures of these two motifs are, indeed, different. Additional chemical modification (4) and temperature gradient gel electrophoresis studies (8) are currently underway to identify the exact nature of these differences and their possible functional implications for future CVd-III mutagenesis.

One striking result of mutagenizing the putative loop E motif of CVd-IIIb was the appearance of wild-type CVd-IIIa among the progeny. Studies of several naturally occurring citrus viroid complexes have shown CVd-IIIa and CVd-IIIb to be the most abundant components of the CVd-III qua-

sispecies (12), but the evolutionary relationship between these two variants has been unclear. It is possible that mutations at 2-3 critical positions in CVd-IIIb create an evolutionary bottleneck that favors the appearance of CVd-IIIa via a coordinated series of sequence changes; alternatively, unsuspected contamination of the mutagenized CVd-IIIb inoculum with traces of wild-type CVd-IIIa could be responsible. Further experimentation to resolve this uncertainty is currently underway.

If this result proves to be real, we would like to know whether or not the process is reversible; i.e., will mutagenesis of CVd-IIIa result in the appearance of the CVd-IIIb? If, on the other hand, our inocula were contaminated, then the variants created by mutagenesis of positions 189-191 must have been much less fit than wild-type CVd-III. Mutagenesis of PSTVd loop E has yielded several variants with altered biological properties (15, 24), and by adjusting our mutational strategy based on the structural differences between the respective loop E motifs it should be possible to generate a similar range of variation in CVd-III.

Finally, viroid infections (especially those involving *Citrus exocortis viroid*) have been reported to inhibit root growth and development in citrus (3, 5, 14). The fact that

restricting wetted zone drip irrigation provides an effective means of reducing tree vigor in high density citrus plantings (7) is consistent with this possibility. Though not conclusive, the results of our initial attempt to demonstrate an inhibitory effect of CVd-III infection on root growth under greenhouse conditions were encouraging. Additional studies have subsequently shown a strong correlation between stem caliper and root dry weight for young rootstock plants; thus, it should be possible to reduce the within-treatment variability in future studies by measuring the effects of infection on the increase in dry weight rather than total dry weight as done here. To be most useful, such an assay should be able to detect changes in dry weight accumulation within 2 yr after viroid inoculation. Sensitivity to the possible deleterious effects of viroid-induced dwarfing (18, 23) would also be desirable.

ACKNOWLEDGMENTS

We thank Tina Paul (Fruit Laboratory) for providing the rootstock plants used in our dwarfing trial, access to a Klecko tissue homogenizer, and advice on various aspects of citrus culture. John Clark (Molecular Plant Pathology Laboratory) provided expert technical assistance.

LITERATURE CITED

1. Bar Joseph, M.
1993. Citrus viroids and citrus dwarfing in Israel. *Acta Hort.* 349: 271-276.
2. Branch, A. D., B. J. Benefeld, and H. D. Robertson
1985. Ultraviolet light-induced crosslinking reveals a unique region of local tertiary structure in potato spindle tuber viroid and HeLa 5S RNA. *Proc. Natl. Acad. Sci. USA* 82: 6590-6594.
3. Cohen, M.
1973. Effect of exocortis inoculation on performance of Marsh grapefruit trees on various rootstocks. In: *Proc. 6th Conf. IOCV*, 117-121. IOCV, Riverside, CA.
4. Ehresmann, C., F. Baudin, M. Mougel, P. Romby, J-P. Ebel, and B. Ehresmann
1987. Probing the structure of RNAs in solution. *Nucleic Acids. Res.* 15: 9109-9128.
5. Flores, R. and J.-L. Rodríguez
1981. Altered pattern of root formation on cuttings of *Gynura aurantiaca* infected by citrus exocortis viroid. *Phytopathology* 71: 964-966.
6. Ho, S. N., H. D. Hunt, R. M. Horton, J. K. Pullen, and L. R. Pease
1989. Site-directed mutagenesis by overlap extension using the polymerase chain reaction. *Gene* 77: 59-74.

7. Golomb, A.
1988. High density planting of intensive groves: A challenge and realization. In: *Proc. 6th Int. Citrus Congr.* 921-930.
8. Hu, Y., P. A. Feldstein, J. Hammond, R. W. Hammond, P. J. Bottino, and R. A. Owens
1997. Destabilization of potato spindle tuber viroid by mutations in the left terminal loop. *J. Gen. Virol.* 78: 1199-1206.
9. Hutton, R. J., Broadbent, P., and K. B. Bevington
2000. Viroid dwarfing for high density citrus plantings. *Hort. Rev.* 24: 277-317.
10. Leontis, N. B. and E. Westhof
2003. Analysis of RNA motifs. *Curr. Opin. Struct. Biol.* 13: 300-308.
11. Owens, R. A., S. M. Thompson, P. A. Feldstein, and S. M. Garnsey
2000. Effects of sequence variation on symptom induction by citrus viroid III. In: *Proc. 13th Conf. IOCV*, 254-264. IOCV, Riverside, CA.
12. Owens, R. A., G. Yang, D. Gundersen-Rindal, R. W. Hammond, T. Candresse, and M. Bar-Joseph
2000. Both point mutation and RNA recombination contribute to the sequence diversity of citrus viroid III. *Virus Genes* 20: 243-252.
13. Owens, R. A., S. M. Thompson, P. J. Sieburth, and M. E. Hliff
2002. Limited sequence randomization: Testing a strategy to produce improved viroid dwarfing agents. In: *Proc. 15th Conf. IOCV*, 249-257. IOCV, Riverside, CA.
14. Pompeu, J., Jr., O. Rodriguez, J. T. Sob, J. P. Neves-Jorge, and A. A. Salibe
1976. Behavior of nucellar and old clones of Hamlin sweet orange on Rangpur lime rootstock. In: *Proc. 7th Conf. IOCV*, 96-97. IOCV, Riverside, CA.
15. Qi, Y. and B. Ding
2003. Inhibition of cell growth and shoot development by a specific nucleotide sequence in a noncoding viroid RNA. *Plant Cell* 15: 1360-13274.
16. Rakowski, A., J. A. Szychowski, Z. S. Avena, and J. S. Semancik
1994. Nucleotide sequence and structural features of the Group III citrus viroids. *J. Gen. Virol.* 75: 3581-3584.
17. Schrader, O., T. Baumstark, and D. Riesner
2003. A mini-RNA containing the tetraloop, wobble-pair and loop E motifs of the central conserved region of potato spindle tuber viroid is processed into a minicircle. *Nucleic Acids Res.* 31: 988-998.
18. Semancik, J. S.
2003. Considerations for the introduction of viroids for economic advantage. *Viroids*, A. Hadidi, R. Flores, J. W. Randles, and J. S. Semancik (eds.), 357-362. CSIRO Publishing, Collingwood, Australia.
19. Semancik, J. S., A. G. Rakowski, J. A. Bash, and D. J. Gumpf
1997. Application of selected viroids for dwarfing and enhancement of production of Valencia orange. *J. Hort. Sci.* 72: 563-570.
20. Semancik, J. S., J. A. Bash, and D. J. Gumpf
2002. Induced dwarfing of citrus by transmissible small nuclear RNA (TsnRNA). In: *Proc. 15th Conf. IOCV*, 390-394. IOCV, Riverside, CA.
21. Stasy, R.A., I. B. Dry, and M. A. Rezaian
1995. The termini of a new citrus viroid contain duplications of the central conserved regions from two viroid groups. *FEBS Lett.* 358: 182-184.
22. Vernière, C., X. Perrier, C. Dubois, A. Dubois, L. Botella, C. Chabrier, J. M. Bové, and N. Duran-Vila
2004. Citrus viroids: Symptom expression and effects on vegetative growth and yield of Clementine trees grafted on trifoliolate orange. *Plant Dis.* 88: 1189-1197.
23. Vidalakis, G., D. J. Gumpf, J. A. Bash, and J. S. Semancik
2004. Finger imprint of *Poncirus trifoliata*: A specific interaction of a viroid, a host, and irrigation. *Plant Dis.* 88: 709-713.
24. Wassenegger, M., R. L. Spieker, S. Thalmeir, F.-U. Gast, L. Riedel, and H. L. Sanger
1996. A single nucleotide substitution converts potato spindle tuber viroid (PSTVd) from a noninfectious to an infectious RNA for *Nicotiana tabacum*. *Virology* 262: 191-197.
25. Zuker, M.
2003. Mfold web server for nucleic acid folding and hybridization prediction. *Nucleic Acids Res.* 31: 3406-15.